REVIEW AND STATISTICAL ANALYSIS OF THE USE OF ULTRASONIC VELOCITY FOR ESTIMATING THE POROSITY FRACTION IN POLYCRYSTALLINE MATERIALS

D.J. Roth and S.M. Swickard

National Aeronautics and Space Administration
Lewis Research Center
21000 Brookpark Road
Cleveland, OH 44135

D.B. Stang

Sverdrup Technology, Inc.
NASA Lewis Research Center Group
Cleveland, OH 44135

M.R. DeGuire

Case Western Reserve University
Cleveland, OH 44106

INTRODUCTION

The physical behavior of components manufactured from polycrystalline materials is in many cases directly dependent on the porosity fraction (volume fraction of pores). As examples concerning key properties of technologically-important materials, porosity fraction has been shown to affect (1) the strength, toughness and modulus of structural and refractory materials such as Steel [1], Tungsten [2], SiC [3], Si_3N_4 [3], and Al_2O_3 [3], (2) the strength of nuclear fuel materials such as UO_2 [4-5], (3) the thermal shock behavior and strength of porcelain-based ceramics [6-7], (4) the dielectric and elastic properties of piezoelectric materials such as PZT [8], and (5) the critical current density, diamagnetic response, and modulus of superconducting ceramics such as $YBa_2Cu_3O_{7-x}$ [9-11]. In such cases where physical properties are directly dependent on porosity fraction, the measurement of porosity fraction becomes important in the quality assurance process for the material.

In this study, we consider the ultrasonic velocity measurement method for estimating porosity fraction. Ultrasonic velocity is a relatively simple measurement that requires the material specimen to have one pair of sides flat and parallel. The advantages of this method are that it is nondestructive and measurements can be made on different regions of a single specimen. Smith [2] and Maclean [12] were two of the first researchers to establish empirical correlations between porosity fraction and ultrasonic velocity for polycrystalline materials. The correlations appeared relatively linear over the porosity fraction ranges investigated. Smith's work concerned metallic samples while Maclean's work concerned ceramic samples. Other researchers began to investigate similar correlations with different materials. Here, we review and statistically analyze

Review of Progress in Quantitative Nondestructive Evaluation, Vol. 10B
Edited by D.O. Thompson and D.E. Chimenti, Plenum Press, New York, 1991

these empirical correlations between ultrasonic velocity and porosity fraction for polycrystalline materials.

SEMI-EMPIRICAL MODEL

The velocity of a longitudinal ultrasonic wave traveling in a solid is related to the elastic properties and density of the solid by [13]:

$$V = \frac{[E(1 - \nu)]}{[\rho(1 + \nu)(1 - 2\nu)]}^{1/2} \quad (1)$$

where V, E, ρ, and ν are the velocity, elastic modulus, bulk density, and Poisson's ratio, respectively, of the material.

An "apparent" modulus [3] for porous materials can be considered which depends on the porosity fraction. Several early empirical investigations provided evidence that the modulus increases exponentially with decreasing porosity fraction according to [14-15]:

$$E = E_o \exp(-bP') \quad (2)$$

where E_o is the elastic modulus of a fully-dense (nonporous) material, b is an empirically-determined constant related to pore shape, pore distribution, and the ratio of open-to-closed pores, and P' is the porosity fraction. The use of Eq. (2) to evaluate E_o by extrapolation from fitted experimental data has sometimes resulted in large discrepancies between the extrapolated and observed values [16]. An alternative to Eq. (2) has been suggested to describe the relationship between elastic modulus and porosity fraction [17]:

$$E = E_o(1 - P')^{2n+1} \quad (3)$$

where n, like b, is an emprically-determined constant that depends on pore distribution and pore geometry factors.[1]

Porosity fraction, P', can be expressed as:

$$P' = \left(1 - \frac{\rho}{\rho_o}\right) \quad (4)$$

where ρ_o is the theoretical (nonporous material) density. Rearranging Eq. (4) allows us to express bulk density as a function of porosity fraction:

$$\rho = \rho_o(1 - P') \quad (5)$$

Substituting Eqs. (3) and (5) into Eq. (1) allows velocity to be expressed as:

$$V = V_o(1 - P')^n \quad (6)$$

---

[1]Concerning the relationship between Poisson's ratio and porosity fraction, most of the limited studies of Poisson's ratio show it decreasing with increasing porosity fraction less rapidly than for elastic modulus [3]. In this development, it is assumed that Poisson's ratio is independent of porosity fraction.

where V_o is a constant for a given material equal to:

$$V_o = \left[\frac{E_o(1 - \nu)}{\rho_o(1 + \nu)(1 - 2\nu)}\right]^{1/2} \tag{7}$$

V_o is the velocity in a fully-dense (nonporous) material, i.e., the "theoretical" velocity. The general case for all n can be shown by expanding the right-hand side of Eq. (6) using the binomial theorem [18] so that:

$$V = V_o\left[1 + [n(-P')] + \frac{n(n - 1)(-P')^2}{2!} + \ldots + \frac{n(n - 1) \ldots (n - k + 1)(-P')^k}{k!} + \ldots\right] \tag{8}$$

From the ratio test, Eq. (8) is absolutely convergent for $|P'| < 1$.

Setting $n = 1$ in Eqs. (3) and (8) results in good agreement for a number of materials over a wide porosity fraction range ($0.1 < P' < 0.7$) [17]. In this case, the right-hand side of Eq. (8) is reduced such that:

$$V = V_o(1 - P') \tag{9}$$

Equation (9) shows a linear relationship between velocity and porosity fraction and is the basis for selecting linear regression to analyze the empirical correlations reported in this study.

It is sometimes convenient to discuss the relationship between velocity and percent porosity, %P, where:

$$\%P = (P')100 \tag{10}$$

Solving Eq. (10) for P' and substituting into Eq. (9) gives:

$$V = m(\%P) + V_o \tag{11}$$

where

$$m = -\frac{V_o}{100} \tag{12}$$

Equation (11) shows a linear relationship between V and $\%P$ where m and V_o are the slope and intercept, respectively.

We can also define a "percent theoretical velocity," %TV, where:

$$\%TV = \left(\frac{V}{V_o}\right)100 \tag{13}$$

Solving Eq. (13) for V and substituting into Eq. (11) gives:

$$\%TV = m'(\%P) + 100 \tag{14}$$

where

$$m' = \frac{(m)100}{V_o} \tag{15}$$

Equation (14) shows a linear relationship between %TV and %P where m' and 100 are the slope and intercept, respectively. Presenting the velocity versus porosity fraction relationship in terms of Eq. (14) is essentially a normalization procedure in that the theoretical velocity of a material and the type of wave (longitudinal or shear) used in the velocity measurement are "removed" as variables. From the derivative of Eq. (14), the following quantity can be defined:

$$\frac{1}{m'} = \frac{\Delta\%P}{\Delta\%TV} \tag{16}$$

where Δ is "change in."

STATISTICAL ANALYSIS METHOD

Linear regression analysis and its associated statistics utilized in this study are briefly described here. Linear regression analysis [19] results in predicted slope (m and m' in Eqs. (11) and (14), respectively) and intercept (V_o in Eq. (11)) values that describe the relationship between V (and %TV) and %P. The Pearson product-moment correlation coefficient and level of significance statistics describe the quality of the regression. The correlation coefficient measures the strength of the linear relationship for the sample data. The level of significance, determined by the number of data points and the value of the correlation coefficient, determines an acceptance or confidence region for the regression. A level of significance of 0.025 corresponds to a 95 percent confidence region. The smaller (better) the level of significance, the lower the probability that the value of the correlation coefficient can be attributed to chance.

Confidence intervals for the predicted slope, intercept, and mean velocity values (the mean of further velocity measurements obtained at some %P value) are also presented. The 95 percent symmetric confidence interval was chosen for the analysis. In practical terms, the 95 percent confidence interval means that in 95 percent of the cases, the true value of the parameter will fall within the calculated interval.

REVIEW AND ANALYSIS

V versus %P data were obtained for Al_2O_3 [20-23], MgO [24], porcelain-based ceramics [7,25], PZT [8], SiC [22,26-29], Si_3N_4 [12,30,31], Steel [32], Tungsten [2], UO_2 [33], $(U_{0.30}Pu_{0.70})C$ [34], and $YBa_2Cu_3O_{7-x}$ [11,35-42] in Ref. 43. In this paper, we present as examples data for SiC, Si_3N_4, and Steel in Tables 1 and 2 and Fig. 1.

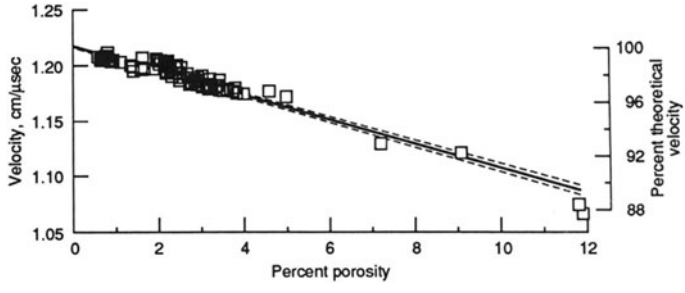

Fig. 1. - Longitudinal velocity versus percent porosity for SiC (ref. 29).

TABLE I.—ULTRASONIC VELOCITY VERSUS PERCENT POROSITY: REVIEW AND STATISTICAL ANALYSIS

Material Reference	Velocity Measurement Technique	Density Measurement Technique	Predicted Line Equation ($V = \beta_1 \cdot \%P + \beta_0$)	Predicted Line Equation ($\%TV = \beta'_1 \cdot \%P + \beta'_0$)	Correlation Coefficient Level of Significance	95% Confidence Intervals for Predicted Intercept (β_0) and Slope (β_1)	95% Confidence Intervals for Predicted Intercept (β'_0) and Slope (β'_1)	$\frac{\Delta\%\ Porosity}{\Delta\%\ Velocity}$
$\frac{\alpha\text{-SiC}}{29}$	Pulse-echo overlap, Longitudinal waves, 20 MHz	Dry-wt. dimensional	LV = −0.011 • %P + 1.22	%TV = −0.883 • %P + 100	$\frac{-0.957}{0.0001}$	$1.22 \le \beta_0 \le 1.22$ $-0.011 \le \beta_1 \le -0.010$	$99.9 \le \beta'_0 \le 100$ $-0.939 \le \beta'_1 \le -0.832$	−1.13
$\frac{Si_3N_4}{12}$	Thru-transmission transit time, Longitudinal waves, 5 MHz		LV = −0.016 • %P + 1.14	%TV = −1.41 • %P + 100	$\frac{-0.997}{0.0001}$	$1.12 \le \beta_0 \le 1.16$ $-0.017 \le \beta_1 \le -0.015$	$98.6 \le \beta'_0 \le 101$ $-1.48 \le \beta'_1 \le -1.34$	−0.71
Steel A-direction (See ref.) 32	Thru-transmission pulse-echo overlap, Dry coupling, Longitudinal waves, 1.5-2.25 MHz	ASTM B-328-60	LV = −0.007 • %P + 0.563	%TV = −1.19 • %P + 100	$\frac{-0.972}{0.0001}$	$0.551 \le \beta_0 \le 0.574$ $-0.007 \le \beta_1 \le -0.006$	$98.0 \le \beta'_0 \le 102$ $-1.32 \le \beta'_1 \le -1.06$	−0.84

The following are abbreviations that appear in the table and their definitions:

V = Velocity (cm/μsec)
LV = Longitudinal wave velocity (cm/μsec)
%TV = Percent theoretical velocity
%P = Percent porosity
β_0 = Predicted value of intercept (Theoretical velocity)
β'_0 = Predicted value of intercept (Percent theoretical velocity)
β_1 = Predicted value of slope (Velocity/percent porosity)
β'_1 = Predicted value of slope (Percent theoretical velocity/percent porosity)
Δ = Change in

Table 1 presents the linear regression statistics corresponding to the scatter plots. The 95 percent confidence interval for the predicted slope and intercept values are presented in the table while the 95 percent confidence interval for mean predicted velocity values is shown by dashed lines on the scatter plots. The quantity (Δ%P/Δ%TV) is provided for the plot lines in the corresponding table entries. (Note that this quantity also has a confidence interval associated with it, the width of which is similar to that for m').

DISCUSSION

General Observations

Concerning the scatter plots given in Ref. 43, correlation coefficients with magnitudes greater than 0.95 were obtained in 28 out of 38 cases. Levels of significance with magnitudes less than 0.025 were obtained in 31 out of 38 cases. For longitudinal wave velocity, predicted intercepts (V_0) ranged from 0.443 cm/μsec for unpoled PZT4 and unpoled PZT5 of Ref. 8 to 1.23 cm/μsec for SiC of Ref. 27. For shear wave velocity, predicted intercepts (V_0) ranged from 0.313 cm/μsec for $YBa_2Cu_3O_{7-x}$ to 0.786 cm/μsec for SiC of Ref. 22. The quantity (Δ%P/Δ%TV) ranged from -0.52 for porcelain of Ref. 7 and poled PZT4 of Ref. 8 to -8.26 for porcelain T2 of Ref. 25. It is understandable that these quantities vary from one material to the next since each material has different elastic properties and density (see Eq. (1)). Predicted intercepts (V_0) and slopes for a specific material from different investigations agree fairly well.

Table 2 compares V_0 predicted from regression analysis with that calculated from Eq. (7) for SiC, Si_3N_4, and Steel. Values of elastic modulus, Poisson's ratio, and density for fully-dense (single crystal and/or polycrystalline) materials used in the calculation are presented. For all cases presented in Ref. 43, the values of V_0 predicted from regression and those obtained from calculation agree within approximately 17 percent in 16 out of 16 cases, and within approximately 5 percent in 8 out of 16 cases.

TABLE II.—COMPARISON OF V_o PREDICTED FROM REGRESSION ANALYSIS WITH THAT CALCULATED FROM EQUATION 7

		Longitudinal Wave Velocity			Values substituted into eq. (7) to obtain V_{oc}		
Material	Single crystal (S) or polycrystalline (P)	Average V_o from regression (V_{or}) [cm/μsec]	Calculated V_o from eq. (7) (V_{oc}) [cm/μsec]	% Variation between V_{oc} and V_{or} $= \{100(\lvert V_{oc} - V_{or} \rvert / V_{oc})\}$	E_o (x 10-6) psi /(ref.)	ν/(ref.)	ρ_o (g/cm^3)
SiC	S		1.16	5.5	58.2/(Ref. 3)	0.17/(Ref. 45)	3.22
	P	1.22	1.22	0.0	64.6/(Ref. 3)	0.17/(Ref. 45)	3.22
Si_3N_4	P	1.12	0.977	15.4	40.0/(Ref. 3)	0.22/(Ref. 3)	3.30
Steel	P	0.580	0.614	5.5	29.0/(Ref. 44)	0.33/(Ref. 44)	7.85

Other Microstructural Variables Affecting Velocity

Although porosity fraction seems to be a significant and perhaps the major microstructural feature affecting ultrasonic velocity, several references point to other microstructural variables having an impact on velocity. These include slight compositional variations [25], preferred domain orientation [8], particle contact anisotropy [32], pore size distribution and geometry [2], and type of agglomeration [21]. These variables may result in differences in predicted intercept (V_O) and slope for what is believed to be the same material from different investigations. Thus, the authors feel that the most accurate and precise application of the ultrasonic velocity method for estimating porosity fraction first requires the development of accurate velocity versus porosity fraction relationships/calibrations for the specific material of interest.

Ramifications

The estimation of batch-to-batch, sample-to-sample and within-sample %P variations for a material can be accomplished if the quantity (Δ%P/Δ%TV) is known with reasonable confidence for that material. The nondestructive mapping of spatial porosity fraction variations within a sample by means of an ultrasonic scanning technique have been reported recently [46-47]. This approach may also be useful in the analysis of the uniformity of composite materials [28].

CONCLUSION

A review and statistical analysis of the ultrasonic velocity method for estimating the porosity fraction in polycrystalline materials is presented. First, a semi-empirical model was developed showing the origin of the linear relationship between ultrasonic velocity and porosity fraction. As examples, velocity versus percent porosity data were shown for SiC, Si_3N_4, and Steel. Linear regression analysis produced slope, intercept, correlation coefficient, level of significance, and confidence interval statistics for the data. Velocity values predicted from regression analysis for fully-dense materials are in good agreement with those calculated from elastic properties. The estimation of batch-to-batch, sample-to-sample, and within-sample variations in porosity fraction for a material can be accomplished from ultrasonic velocity measurements if reasonable confidence exists in the velocity versus percent porosity linear relationship.

REFERENCES

1. G.C. Goetzel, Treatise on Powder Metallurgy, (Wiley, New York, 1963).
2. J.T. Smith, and S.A. LoPilato, Trans. Metall. Soc. AIME, 236, 597 (1966).
3. R.W. Rice, Treatise on Materials Science and Technology, Vol. 11, Properties and Microstructure, R.K. MacCrone, ed., (Academic Press, New York, 1977), p. 203.
4. F.P. Knudsen, H.S. Parker, and M.D. Burdick, J. Am. Ceram. Soc., 43, 641 (1960).
5. M.D. Burdick and H.S. Parker, J. Am. Ceram. Soc., 39, 181 (1956).
6. E.C. Williams, R.C. Reid-Jones, and D.T. Dorrill, Trans. Brit. Ceram. Soc., 62, 405 (1963).
7. J. Boisson, F. Platon, and P. Boch, Ceramurgia, VI (2), 74 (1976).
8. N.D. Patel and P.S. Nicholson, Am. Ceram. Soc. Bull., 65, 783 (1986).
9. N.McN. Alford, W.J. Clegg, M.A. Harmer, J.D. Birchnall, K. Kendall, and D.H. Jones, Nature, 332, 58 (1988).
10. S.N. Song, S.-J. Hwu, F.I. Du, K.R. Poeppelmeir, T.O. Mason, and J.B. Ketterson, Adv. Ceram. Mater., 2, 480 (1987).
11. J.E. Blendell, et al., Adv. Ceram. Mater., 2, 512 (1987).
12. A.F. McLean, A.E. Fisher, R.J. Bratton, and D.G. Miller, "Brittle Materials Design, High Temperature Gas Turbine," AMMRC-CTR-75-8, Apr. 1975, p. 97. NOTE: THIS DOCUMENT IS RESTRICTED.
13. J. Szilard, ed., Ultrasonic Testing, (Wiley, New York, 1982), p. 5.
14. E. Ryshkewitch, J. Am. Ceram. Soc., 36, 65 (1953).
15. R.M. Spriggs, J. Am. Ceram. Soc. 44, 628 (1961).
16. I. Soroka and P.J. Sereda, J. Am. Ceram. Soc., 51, 337 (1968).
17. K.K. Phani and S.K. Niyogi, J. Mater. Sci. Lett., 5, 427 (1986).
18. E.W. Swokowski, Calculus With Analytic Geometry, (Prindle, Weber & Schmidt, Boston, MA, 1975) P. 761.
19. F.S. Acton, Analysis of Straight Line Data, (Wiley, New York, 1959).
20. T.N. Claytor, H.M. Frost, T.H. Feiertag, G.A. Sheppard, and P.D. Shalek, Mater. Eval., 47, 532 (1989).
21. M.P. Jones, G.V. Blessing, and C.R. Robbins, Mater. Eval., 44, 859 (1986).
22. D.S. Stang, Unpublished research, NASA Lewis Research Center, Cleveland, OH, 1989.
23. R.M. Arons and D.S. Kupperman, Mater. Eval., 40, 1076 (1982).
24. D.S. Kupperman and H.B. Karplus, Am. Ceram. Soc. Bull., 63, 1505 (1984).
25. K.G. Shyuller, G.V. Khennike, and Z.D. Kovziridze, Glass Ceramics, 44, 473 (1988).
26. W.D. Friedman, R.D. Harris, P. Engler, P. K. Hunt, and M. Srinivasan, Nondestructive Testing of High Performance Ceramics, A. Vary and J. Snyder, eds., (American Ceramic Society, Columbus, OH, 1987), p. 128.
27. G.Y. Baaklini, E.R. Generazio, and J.D. Kiser, J. Am. Ceram. Soc., 72, 383 (1989).
28. J.J. Gruber, J.M. Smith, and R.H. Brockelman, Mater. Eval., 46, 90 (1988).
29. S.J. Klima, G.K. Watson, T.P. Herbell, and T.J. Moore, Ultrasonic Velocity for Estimating Density of Structural Ceramics. NASA TM-82765, 1981.
30. T. Derkacs, I.M. Matay, W. D. Brentnall, Nondestructive Evaluation of Ceramics. TRW-ER-7798-F, TRW Inc., Cleveland, OH, May 1976, (Avail. NTIS, AD-A027357).
31. J.S. Thorp and T.G. Bushell, J. Mater. Sci. 20, 2265 (1985).
32. E.P. Papadakis and B.W. Petersen, Mater. Eval. 37 (5), 76 (1979).
33. J.P. Panakkal and J.K. Ghosh, J. Mater. Sci. Lett., 3, 835 (1984).

34. J.K. Ghosh, J.P. Panakkal, and P.R. Roy, World Conference on Nondestructive Testing, (Butterworths, Stoneham, MA, 1985), p. 1201.
35. A.L. Gaiduk, et al., Sov. J. Low Temp. Phys., 14, 395 (1988).
36. D.J. Roth, E.R. Generazio, D.B. Stang, and A.F. Hepp, Subtle Porosity Variation in the $YBa_2Cu_3O_{7-x}$ Superconductor Revealed by Ultrasonic Imaging. NASA TM-102130, 1990.
37. S. Ewert, et al., Solid State Commun. 64, 1153 (1987).
38. V. Ramachandran, G.A. Ramadass, and R. Srinivasan, Physica C, 153, 278 (1988).
39. M. Suzuki, Y. Okuda, I. Iwasa, A. J. Ikushima, T. Takabatake, Y. Nakazawa, and M. Ishikawa, Physica C, 153, 266 (1988).
40. K.J. Sun, M. Levy, B.K. Sarma, P.H. Hor, R.L. Meng, Y.Q. Wang, and C.W. Chu, Phys. Lett. A, 131, 541 (1988).
41. H.M. Ledbetter, M.W. Austin, S.A. Kim, and M. Lei, J. Mater. Res., 2, 786 (1987).
42. R. Round and B. Bridge, J. Mater. Sci. Lett., 6 1471 (1987).
43. D.J. Roth, D.B. Stang, S.M. Swickard, and M.R. DeGuire, Review and Statistical Analysis of The Ultrasonic Velocity Method For Estimating The Porosity Fraction in Polycrystalline Materials. NASA TM-102501, 1990.
44. G.E. Deiter, Mechanical Metallurgy, 3rd ed., (McGraw-Hill, New York, 1986), p. 50.
45. Engineering Property Data On Selected Ceramics, Vol. 2, Carbides, (Metals and Ceramics Information Center, Battelle's Columbus Laboratories, Columbus, OH, 1979), p. 5.2.3-10.
46. E.R. Generazio, D.J. Roth, and G.Y. Baaklini, Mater. Eval. 46. 1338 (1988).
47. E.R. Generazio, D.J. Roth, and D.B. Stang, J. Am. Ceram. Soc., 72, 1282 (1989).